Annales de Paléontologie 109 (2023) 102629

Disponible en ligne sur
ScienceDirect
www.sciencedirect.com

Elsevier Masson France
EM|consulte
www.em-consulte.com

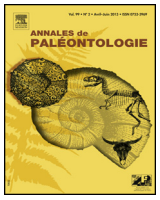

Original article

Biotic vs abiotic origin of unusual features from Mesoproterozoic of Vindhyan Supergroup, India

Origine biogénique vs *abiogénique de structures atypiques du Mésoprotérozoïque du supergroupe de Vindhyan, Inde*

Adrita Choudhuri [a], Abderrazak El Albani [b,*], Sabyasachi Mandal [a], Subir Sarkar [c]

[a] *Birbal Sahni Institute of Palaeosciences, 226007 Lucknow, India*
[b] *University of Poitiers, UMR-CNRS-IC2MP 7285, 86073 Poitiers, France*
[c] *Department of Geological Sciences, Jadavpur University, 700032 Kolkata, India*

ARTICLE INFO

Article history:
Received 25 May 2023
Accepted 12 August 2023

Keywords:
Biosphere
MRS
Chorhat Sandstone
Boring Billion
Vindhyan
Biotic or abiogenic

ABSTRACT

Biogenic signatures in Precambrian rocks are often difficult to confirm and debatable. We present some unusual features associated with microbial-mat related structures (MRS) from the freshly-exposed rippled bed surface of 1.6 Ga old Chorhat Sandstone, Vindhyan Supergroup, India. The features discussed here, are present within intertidal to supratidal environments often affected by storms. One of the features includes ridge-groove couplets that run across the ripple crests. Locally, the ridge-groove couplet forms a braid-like pattern. Along the ripple troughs, the ridges are considerably long and maintain a uniform width on the mm scale. Another feature shows meandering grooves bordered by ridges. The grooves swerve, form loops, cut across older grooves, and branch up. None of them have comparable equivalents in the Precambrian record described thus far. The invariably uniform width of the ridges for both the two features cannot be compared with undersurface gas bubble migration, and the swerving and reversing nature of the grooves denies passive movement of any inorganic/organic masses under the influence of an external force. They seem to have been created by movement through a microbiota-rich surficial sediment. Such unusual features raise questions about the biosphere and biotic structures during the Boring Billion (1.8–0.8 Ga).

© 2023 Elsevier Masson SAS. All rights reserved.

Mots clés :
Biosphere
Tapis microbiens
Grès de Chorhat
« Boring billion »
Vindhyan
Biogénique ou abiogénique

RÉSUMÉ

Les signatures biogéniques dans les roches précambriennes sont souvent difficiles à confirmer et elles sont très régulièrement débatues. Dans ce travail, nous présentons des structures inhabituelles associées aux tapis microbiens (MRS) ondulés et localisés à la surface des bancs de grès de Chorhat vieux de 1,6 Ga, bien preservés et appartenant au Supergroupe de Vindhyan, Inde. Les caractéristiques discutées sont décrites comme relevant d'environnements intertidaux à supratidaux souvent affectés par des courants de tempêtes. L'une de ces caractéristiques comprend des couplets de crêtes-rainures qui traversent des crêtes d'ondulation. Localement, le couple crêtes-rainures forme un motif en forme de tresse. Le long des creux ondulés, les crêtes sont considérablement longues et conservent une largeur uniforme à l'échelle du millimètre. Une autre caractéristique montre des rainures sinueuses bordées de crêtes. Les rainures s'écartent, forment des boucles, coupent les rainures plus anciennes et se ramifient. Aucun d'entre elles n'a d'équivalents comparables dans les archives précambriennes décrites jusqu'à présent. La largeur invariablement uniforme des arêtes pour les deux caractéristiques ne peut être comparée à la migration des bulles de gaz sous la surface. En plus, la nature déviée et inversée des rainures empêche le mouvement passif de toute masse inorganique/organique sous l'influence d'une force externe. Ils semblent avoir

* Corresponding author.
E-mail address: abder.albani@univ-poitiers.fr (A. El Albani).

https://doi.org/10.1016/j.annpal.2023.102629
0753-3969/© 2023 Elsevier Masson SAS. All rights reserved.

été formées par mouvement à travers un sédiment superficiel riche en microbiota. Ces caractéristiques inhabituelles soulèvent des questions à propos de la biosphère et les structures biotiques au cours du « Boring Billion » (1,8–0,8 Ga).

© 2023 Elsevier Masson SAS. Tous droits réservés.

1. Introduction

The composition of the Proterozoic biosphere remains largely uncertain due to the scarcity of an unequivocal Precambrian palaeobiological record. The recovery of benthic microfossils has provided some guidance for understanding the trajectory of evolution (Butterfield, 2007; Knoll, 2014). Evidence for complex macroscopic (e.g., metazoan) life before the Ediacaran (635–539 Ma) has long been controversial. There is a consensus that motile eukaryotes became commonplace only after the Neoproterozoic Oxygenation Event (NOE) (Canfield et al., 2007, 2008; Carbone and Narbonne, 2014; Chen et al., 2019; Och and Shields-Zhou, 2012; Scott et al., 2008; Shields-Zhou and Och, 2011). However, the earliest record of biomarkers typically belonging to eukaryotes comes from rocks as old as 2.7 Ga (Brocks et al., 1999; Summons et al., 1999). The recent discovery of the oldest record of motile eukaryotes from a 2.1 Ga old formation in Gabon documents the horizontal movement through glide that was produced during mat mining and burrowing (El Albani et al., 2019) and reasonably occurred in relation to the Great Oxygenation Event (GOE) (Lyons et al., 2014; Chen et al., 2020; Large et al., 2022; López-García and Moreira, 2008, 2021; Mänd et al., 2020). Molecular clock estimates of the initial divergence of metazoans based on molecular sequence date as far back as Cryogenian times (Cunningham et al., 2017; Donoghue and Benton, 2007; dos Reis et al., 2015; Erwin, 2015, 2020; Erwin et al., 2011; Lozano-Fernandez et al., 2017; Peterson et al., 2004, 2008; Pisani and Liu, 2015).

In contrast to the Paleoproterozoic and Neoproterozoic, the Mesoproterozoic, the so-called "Boring Billion" Era, witnessed very few tangible records of advanced life forms(Bengtson et al., 2009; Rasmussen et al., 2002a; Seilacher et al., 1998). This billion-year time interval (1.8 Ga to 0.8 Ga) between the GOE and NOE is considered a period of geobiological stasis (Brasier and Lindsay, 1998; Buick et al., 1995; Mukherjee et al., 2018). It is often inferred that a drop in atmospheric oxygen level and a limited distribution of trace elements severely hindered eukaryotic evolution during this period(Anbar and Knoll, 2002; Partin et al., 2013; Robbins et al., 2016; Scott et al., 2008). However, a thick microbial mat could have acted as an "oxygen mask" in otherwise poorly-oxygenated Mesoproterozoic oceans(Gingras et al., 2011; Seilacher, 1999). Thus, the surficial ocean water may have been rich in oxygen and other essential bionutrients (Anbar and Knoll, 2002). The Mesoproterozoic Era is believed to mark a time with no evolutionary novelties in terms of macroscopic eukaryotes. Although some examples exist, they are generally referred to as "pre-Ediacaran dubio fossils" (Rasmussen et al., 2002a; Seilacher et al., 1998; Seilacher, 2007). Bengtson et al. (2007) also reported trace fossils among the 1.8 Ga-old Stirling Formation. They concluded that such significant traces are not necessarily megascopic life forms, as simpler multicellular organisms can produce them (Bengtson and Rasmussen, 2009; Matz et al., 2008).

In this sense, the Mesoproterozoic Vindhyan Supergroup (Indian Peninsula) has always been of global interest due to its potential for studies on the evolution of life during the "Boring Billion" period. Large varieties of microfossils, stromatolites, carbonaceous fossils, Ediacaran fossils, and traces of metazoans have been recorded by several studies from the Vindhyan succession (Bengtson et al., 2009; Choudhuri et al., 2020; De, 2006; Javaux and Lepot, 2018; Sarkar and Banerjee, 2020; Sharma and Shukla, 2009; Srivastava, 2012). However, the ubiquitous presence of microbial-mat related structures (MRS) within multiple siliciclastic horizons of the Vindhyan Supergroup (Eriksson et al., 2010; Sarkar et al., 2006), as well as their morphological diversity, provide an opportunity to consider claims of the presence of body fossils and macroscopic life (Choudhuri et al., 2020; Sarkar and Banerjee, 2020; Srivastava, 2012). In addition to the biogenicity issue, the present work is relevant to the understanding of the timing related to the emergence of eukaryotes, which is largely believed to have occurred during the Mesoproterozoic (~1.6 Gy ago) and suspected to have emerged significantly earlier (Javaux and Lepot, 2018; Knoll, 2014). Here, we describe and discuss some new, exceptionally-preserved and unusual bedding plane structures (BPSs) from the 1.6 Ga old and MRS-rich Chorhat Sandstone, Vindhyan Supergroup, India. Additionally, we critically evaluate their origins, such as the possible biological behaviours or motions of artefacts affecting the bedding plane, based on detailed morphological analysis.

2. Geological background

The Vindhyan Basin in central India is the second largest Proterozoic basin in the world and is only slightly metamorphosed and deformed (Fig. 1A) (Bickford et al., 2017; Bose et al., 2001; Sarkar and Banerjee, 2020). **The sedimentary rocks of the basin were i**nitially interpreted as marine, but now the basin is known to contain a significant proportion of terrestrial deposits as well (Bose and Chakraborty, 1994; Sarkar et al., 2011). A basin-wide unconformity, presumably a hiatus of ~400 Ma (Tripathy and Singh, 2015), separates the Lower Vindhyan/Semri Group from the Upper Vindhyan Group (Fig. 1B) (Bose et al., 2001; Mandal et al., 2019, 2022). The studied BPSs discussed in this paper are present in the Chorhat Sandstone Member belonging to the Kheinjua Formation (Fig. 1B). It gradationally overlies the Koldaha Shale of marine shelf origin (Fig. 1B) (Bose et al., 2001). The pyroclastics from the Porcellanite Formation underlying the Kheinjua Formation are constrained to 1628± 8 Ma based on U/Pb and Pb/Pb ratios (Fig. 1B) (Bickford et al., 2017; Rasmussen et al., 2002b). On the other hand, the Chorhat Sandstone is sharply overlain by the shelf-originated Rampur Shale, where pyroclastic rocks are also dated on the same basis as 1599 ± 8 Ma (Fig. 1B)(Rasmussen et al., 2002b). Between the Porcellanite Formation below and the Rampur Shale Member above, the age of the Chorhat Sandstone Member should be between 1628 ± 8 Ma and 1599 ± 8 Ma (Fig. 1B) (Rasmussen et al., 2002b). The grey-coloured Koldaha Shale was deposited on a shelf that gradually shows a regressive pattern and transitions into the coarsening-upwards ~65 m-thick Chorhat Sandstone. It consists mostly of of sandstones intersparsed with red-coloured silt/mudstone that are interpreted as Highstand System Tract (HST; Fig. 1B) (Sarkar et al., 2006). The Chorhat Sandstone consists of alternate storm beds with hummocky cross-stratification (HCS), testifying to a storm-dominated platform. This member evolves upwards to supratidal facies (Sarkar et al., 2014) testifying to sedimentary environments dominated by tidal dynamics.

Two facies associations are found to constitute the Chorhat Sandstone Member. The lower facies association (maximum thick-

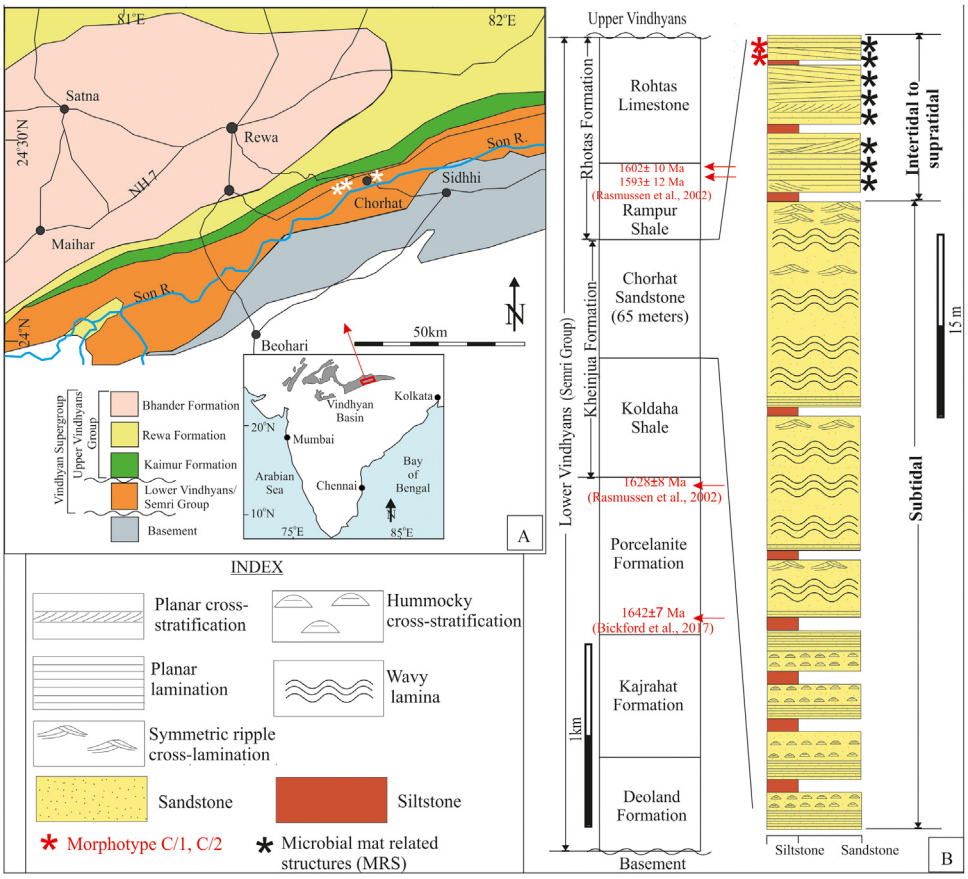

Fig. 1. Simplified geological map and stratigraphic framework of the studied interval. A. Geological map of the study area showing the geological units of the Vindhyan Supergroup (inset map shows the position of the Vindhyan Basin within a map of India) and the outcrop locations near Chorhat village (white asterisks). B. General stratigraphic framework of the Lower Vindhyan (to the left). The stratigraphic column (to the right) shows the vertical facies stacking and the position of the MRS (black asterisks) and **morphotypes C/1** and **C/2** discussed in the paper (red asterisks).
Carte géologique simplifiée et cadre stratigraphique de l'intervalle étudié. A. Carte géologique de la zone d'étude montrant les unités géologiques du supergroupe de Vindhyan (le cadre montre la position du bassin de Vindhyan sur une carte de l'Inde) et les emplacements des affleurements près du village de Chorhat (astérisques blancs). B. Cadre stratigraphique général du Bas Vindhyan (à gauche). La colonne stratigraphique (à droite) montre l'empilement vertical des faciès et la position des tapis microbiens (astérisques noirs) et des morphotypes C/1 et C/2 discutés dans l'article (astérisques rouges).

ness of 20 m) is characterised by vertical stacking of 35–40 cm thick tabular beds of light-coloured fine-grained sandstone, alternating with siltstone interbeds that are less than 5 cm thick. The individual sandstone beds are often thin ($\leq$ 5 cm), but the thicker beds are massive overall. Amalgamation of the sandstone beds is common (Fig. 2A). The thick sandstone beds have sharp erosional bases riddled with gutters and prod marks. Internally, these thick sandstone beds are often characterised by hummocky cross-stratification (HCS) (Fig. 2B). Wave ripples with straight or broadly-sinuous and locally-bifurcating crests generally mantle these sandstone beds (Fig. 2C). All these features indicate that they were deposited within the storm wave base (Grundvåg et al., 2021; Sarkar et al., 2006, 2014). The upper facies association (maximum thickness of 45 m) is characterised by mudstone beds interbedded with well-sorted, fine- to medium-grained, symmetrical ripple cross-laminated sandstone. The sandstone beds are mostly thicker than 10 cm, and the sandstone beds gradually increases towards the top (Fig. 1B). Mudstone beds interbedded with sandstone indicate mud deposition took place in a low energy environment, possibly within the intertidal zone, and sand beds were deposited there by storms. Reddish-coloured mudstone clasts often present along the foresets of cross-bedded sandstone (Fig. 2D) confirms the storm-origin of the sandstone beds. Smaller ripples migrating along the troughs of larger ripples (Fig. 2E) as well as the superimposition and interference of ripples on sandstone bed surfaces signifies an intertidal setting. At the top (2 m) of the upper facies association that immediately underlies the Rampur Shale Member, the sandstone bed surfaces often bear desiccation features (Fig. 2F) and salt pseudomorphs. The depositional surfaces are intermittently subaerially exposed (Fig. 2F). This indicates that the palaeodepositional environment was gradually shallowing upwards from an intertidal to a supratidal zone (Sarkar et al., 2014, 2006). Diverse types of MRS are spectacularly preserved on the storm-derived sandstone bed surfaces in both the lower and upper facies associations (Figs. 3 and 4) (Sarkar et al., 2006, 2014, 2016). The preservation of MRS within the well-sorted Chorhat Sandstone favours increased cohesiveness of the sand particles due to the secretion of extracellular polymeric substances (EPS) by microorganisms (Noffke and Awramik, 2013).

3. Materials and methods

The Chorhat Sandstone was studied around the town of Chorhat (Fig. 1A) along a ~12 km stretch of road-cutting. Typical field equipment such as a hammer, chisel, clinometre, GPS, measuring tape, and a camera were used. We documented all sampling spots with photographs and GPS coordinates. A stratigraphic column (Fig. 1B) was prepared using the usual technique along with documentation of facies and MRS (black asterisk in Fig. 1B) present on the bedding surfaces at different stratigraphic levels. Bedding surfaces (red asterisk in Fig. 1B) that preserved the structures (BPSs)

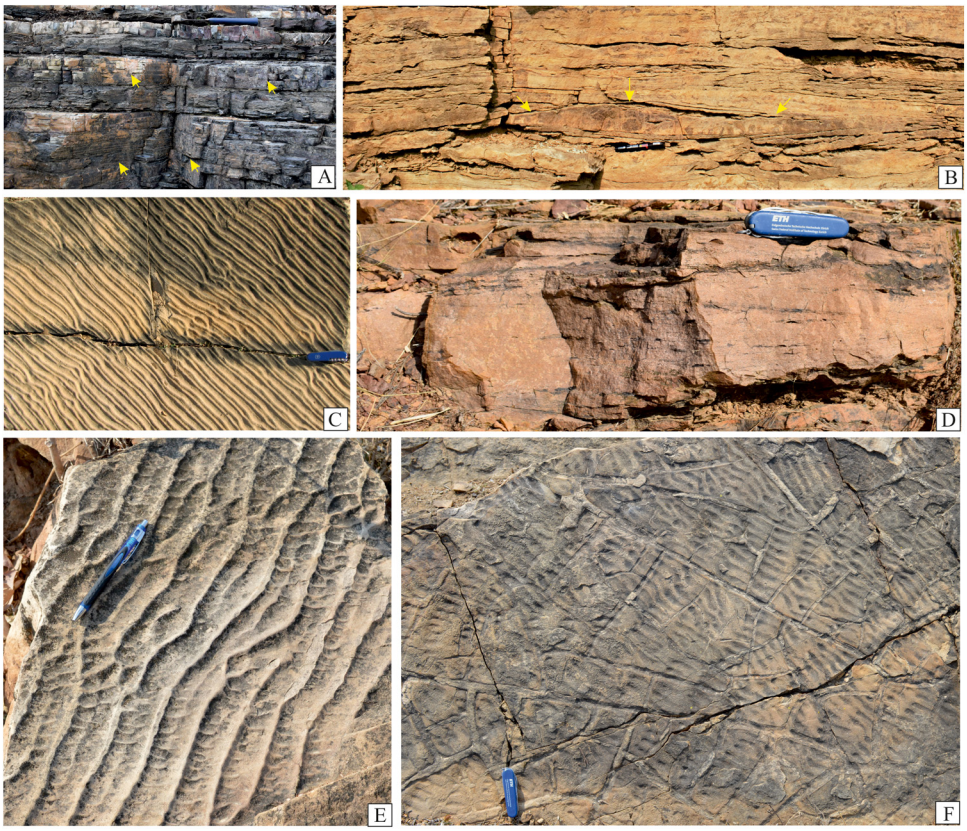

Fig. 2. Field photos of sedimentary structures present within the Chorhat Sandstone Member, Vindhyan Supergroup. A. Amalgamated sandstone beds of storm origin within the Chorhat Sandstone; hammer length = 35 cm. B. Hummocky cross-stratified sandstone (HCS, arrowed); marker length = 15 cm. C. Broadly sinuous and bifurcating crestlines of wave ripples along with median ripples preserved on the sandstone bedsurface; knife length = 8.5 cm. D. Mud clasts are arranged as imbricate shingles within the sandstone. E. Ladder-back ripples are migrating along troughs of the larger ripples. F. Desiccation cracks on the rippled sandstone bed surface.
Photos de terrain montrant des structures sédimentaires situées dans le membre de grès de Chorhat, Supergroupe de Vindhyan. A. Bancs de grès amalgamés de tempestite dans le grès de Chorhat; longueur du marteau = 35 cm. B. Grès montrant des stratifications entrecroisées en mamelons (fléche); longueur du marqueur = 15 cm. C. Lignes de crête largement sinueuses et bifurquantes, des rides de vagues avec des ondulations médianes préservées à la surface des bancs de grès ; longueur du couteau = 8,5 cm. D. Les clastes argileux sont disposés sous forme de lits imbriqués au sein des grès. E. Rides médianes migrantes le long des creux des plus grandes rides. F. Figures de dessication à la surface des rides de bancs de grès.

were cleaned, and overburdens were removed for photographic documentation. Measurements and detailing of the morphological descriptions of the unusual structures were performed on-site during fieldwork. Later, the photographs were used to draw hand sketches on a computer to enhance clarity.

4. Description and interpretation of Chorhat unusual structures

All the unusual structures (BPSs) described below are preserved on the freshly exposed bed surfaces within the top two metres of the coastal (intertidal to supratidal) deposits of the Chorhat Sandstone, Vindhyan Supergroup, India.

4.1. Morphotype C/1: Ridge-groove couplets

4.1.1. Description

This morphotype is found as a positive epirelief on well-sorted, fine-grained, and wave-rippled sandstone (Fig. 5A). It is generally represented by divergent sets of curvilinear ridges with grooves on their concave side. Together, these sets of ridges and grooves form a ~22 cm-long curvilinear band that runs across a ripple train (Fig. 5A). The ridge-groove couplets repeat themselves one after another to constitute the curvilinear pattern of the **morphotype C/1**. Individual curvilinear ridges maintain a uniform width of approximately 2 mm. Their length is mostly about 2 cm, but where they run along the ripple trough, they are longer, up to 8.5 cm (Fig. 5B, white arrow). Length and width measured from both the best preserved example as well as similar ill-developed structures are shown in Fig. 5F. At one point on the curvilinear band, the ridges connect like galleries, giving rise to a braid-like pattern (Fig. 5C). At another end on the same band, ridge-groove couplets emerge from one side of a beaker-like form defined by a single ridge with reverse bending but are not accompanied by any groove (Fig. 5D). At the base of the beaker, smaller ridges run across a ripple crest. On the lee side of the ripple, the ridges are separated by grooves. Still, on the stoss side, the grooves tend to disappear as the ridges flare (Fig. 5D). After this (at the end of a rectangle in Fig. 5A), there are more than four isolated half-moon shaped ridges with asymmetrical grooves (Fig. 5A) and, they decrease gradually in size (Fig. 5A). The rippled sandstone bed surface bears many obvious relicts of similar ridge-groove couplets (indicated by red arrow in Fig. 5C). In addition, numerous relict patches of wrinkle structures are on the wave-rippled surface (Fig. 5E).

4.1.2. Interpretation

The **morphotype C/1** reveals some object, animate or inanimate, resting intermittently on the rippled sediment surface. They represent more than one pattern (braided patterned ridges, isolated half-moon-shaped ridges with asymmetrical grooves, and beakers with a single ridge with no grooves) on a rippled bedding plane. Its curvilinear trackway and repetitive and regular pattern

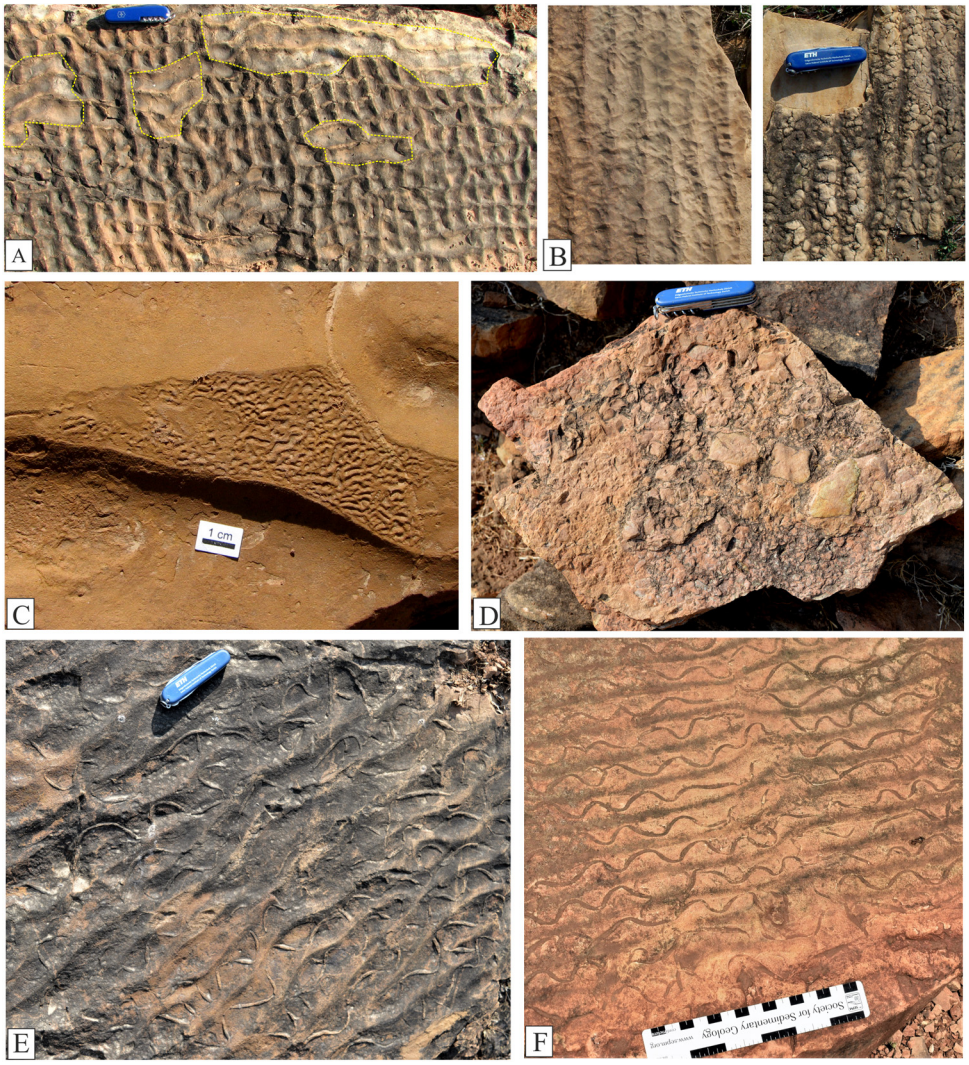

Fig. 3. Different varieties of microbial-mat related structures (MRS) present within the Chorhat Sandstone (positions marked as black asterisks in B). A. Patchy ripples; knife length = 8.5 cm. B. load balls (to the right) and their casts (to the left) preserved on the rippled sandstone bed surface. C. Kinneyia-type wrinkles. D. Sand clasts. E and F. Sand-filled cracks on the rippled sandstone bed surface; scale length = 15 cm.

Différentes variétés de structures liées au tapis microbien (MRS) présentes dans le grès de Chorhat (positions marquées par des astérisques noirs sur la B). A. Rides à dimenssions inégales; longueur du couteau = 8,5 cm. B. figures de charges (à droite) et leurs moulages (à gauche) conservés sur la surface du banc de grès montrant des rides. C. Plissements de type Kinneyia. D. Clastes de sable. E et F. Fissures remplies de sable sur la surface du banc de grès avec des rides ; longueur de l'échelle = 15 cm.

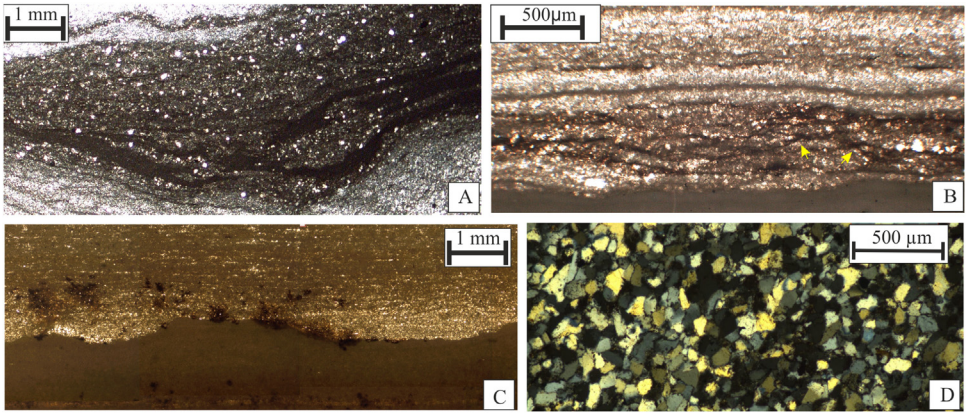

Fig. 4. Optical microscopy of MRS shown in Fig. 3. A. Dark microbial laminae showing wrinkles and fine silt-sized particles trapped within the mat fabric. B. Frayed edges (arrowed) of microbial laminae associated with MRS. C. Dark-colored microbial laminae showing loading overlain by silt-sized particles. D. Sand clasts shown in Fig. 3D reveal the well-sorted and mud-free nature of fine-grained quartz grains.

Microscopie optique des tapis microbiens illustrées au niveau de la Fig. 3. A. lamines microbiennes sombres montrant des rides et de fines particules de la taille de silts fins piégées dans à l'intérieur du tapis. B. Bordures discontinues (fléchés) des lames microbiennes associées aux MRS. C. Lamines microbiennes de couleur sombres montrant une charge recouverte de particules de la taille de silts fins. D. Les clastes de grès illustrés à la Fig. 3D révèlent la nature bien triée et sans paticules fines, des grains de quartz à grains fins.

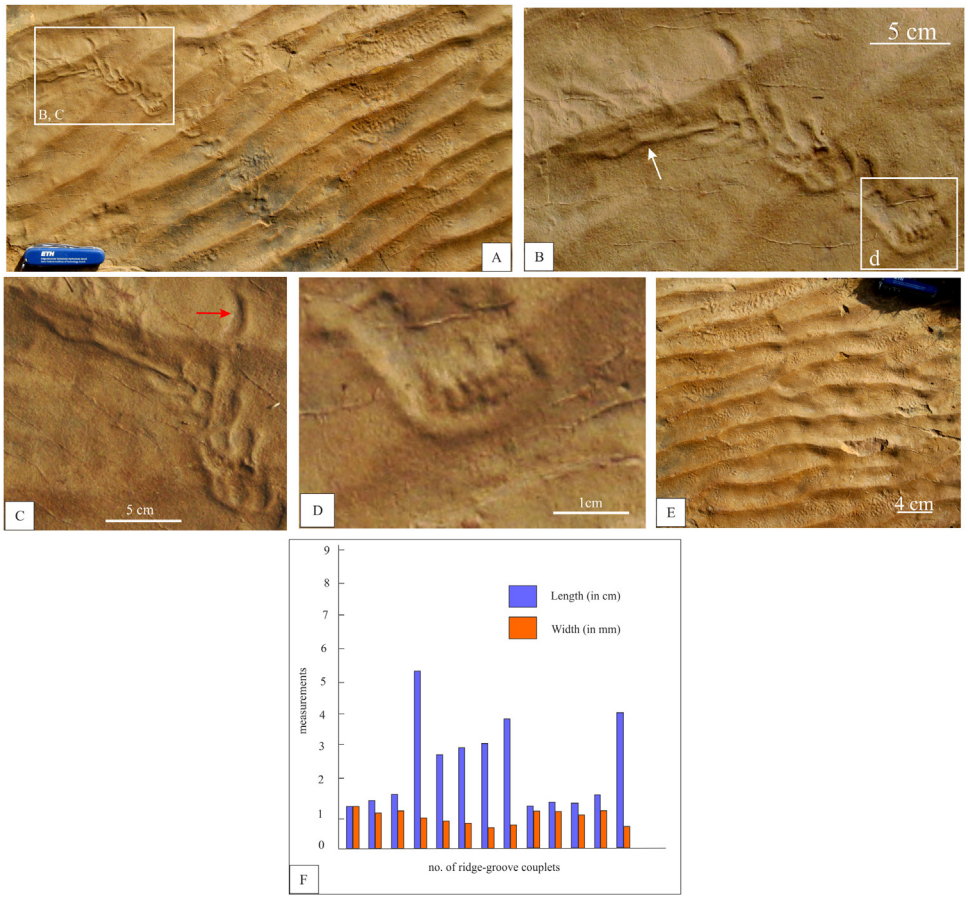

Fig. 5. Field photo of morphotype C/1: Ridge-groove couplets. A. curvilinear row made up of several ridge-groove couplets perpendicularly crossing the wave-rippled bed surface; knife length = 8.5 cm. B. Enlarged part of the white rectangle in 5a showing an individual ridge (longer > 1 cm; white arrow) of uniform width running parallel to the ripple trough. C. Enlarged part of the rectangle marked in A showing ridge-groove couplets crisscrossed in nature, forming a braid-like pattern. D. Enlarged view of a beaker-like form (marked in B) defined by a single ridge with reverse bending. Note that the ridge-groove couplets are found to emerge from one side of the beaker-like form. E. Preserved patches of wrinkle structure within the ripple troughs. F. Histogram showing variable length and width of the ridge-groove couplets forming the **morphotype C/1**.

Photo de terrain du morphotype C/1 : Couplets crête-rainure. A. rangée curviligne composée de plusieurs couplets crête-rainure traversant perpendiculairement la surface du banc présentant des rides de vagues ; longueur du couteau = 8,5 cm. B. Partie agrandie du rectangle blanc en A montrant une crête individuelle (plus longue > 1 cm ; flèche blanche) de largeur uniforme parallèle au creux de rides. C. Partie agrandie du rectangle marqué sur la A montrant des couplets de crête-rainure entrecroisés, formant un motif en forme de tresse. D. Vue agrandie d'une forme en forme de goutière (marquée sur la B) définie par une seule crête avec flexion inversée. Les couplets crête-rainure émergent d'un côté de la structure en forme de « coupole ». E. Zones conservées des structures plissées situées au sein des creux de rides. F. Histogramme montrant la longueur et la largeur variables des couplets crête-rainure formant le morphotype C/1.

(Fig. 5A) point toward its potential biogenicity. An abundance of remnants of isolated half-moon shaped ridges (Fig. 5C, red arrow) in the close vicinity further corroborates this contention. If this feature results from the involuntary movement of an inanimate object, it could be considered a pathway of skip marks (Collinson and Thompson, 1989). This would then suggest that the object had a rugged surface with protrusions in unequal spacing. Superimposition of a weaker current on a strong unidirectional current is attributed to an object that had no self-control over its movement veering from a linear trackway. The general sharpness of ripple crests (Fig. 5A and E), nonetheless, denies the role of any strong current soon after ripple formation. However, since then, no such comparable object with a rugged surface and protrusion is expected from rocks as old as 1.6 Ga. We focus on the **morphotype C/1** in this paper for appropriate interpretation by Precambrian palaeobiologists. Laflamme et al. (2012) described discrete elongated structures generated due to the coalescence of numerous gas bubbles or movement of "bubble trains". Microbial metabolism and decomposition generate gas under mat cover (Choudhuri, 2020), and movement of the gas bubbles under the current-swept mat cover can be invoked to explain the structures under consideration. Numerous relict patches of wrinkle structure in association with the said structure (Fig. 5E) indeed support prolific microbial mat growth. However, the braided-patterned ridges of the **morphotype C/1** (Fig. 5C) differ from the "bubble trains" described by Laflamme et al. (2012) due to the lack of pustulous morphology and uniformity of the ridge width. Compressible gas bubbles are not expected to generate ridges of uniform width, while the movement of organisms is expected. It appears that some objects (e.g., microbial flocs) were dragged or some organisms () were moving under a thin veneer of the microbial biofilm. The movement trackways were connected like galleries, giving rise to braided-patterned ridges (Fig. 5C). The dragging of microbial flocs by wave agitation or the movement of gas bubbles had very little chance to create the interconnected braid-like ridges observed in the **morphotype C/1**. The modern examples shown by Warren et al. also do not match the braid-patterned ridges shown in Fig. 5C (Warren et al., 2020). The interconnected nature of the braided-patterned ridges (Fig. 5C) of the **morphotype C/1** points towards biogenicity. Experiments by Mariotti et al. (2014) and the pseudotraces reported by Warren et al. (2020) from modern-day shallow water environments show that the movement of microbial flocs over the sandy bed surface

under wave action can generate ridge and pit-like structures. Millimetre-sized, lightweight microbial fragments/macro algae can move under wave agitation and generate lumpy structures on sandy surfaces. The half-moon-shaped ridges (at the end of the rectangle in Fig. 5A) could have been generated by the saltation of microbial flocs due to wave agitation over the sandy bed surface, as described by Warren et al. (2020). Smaller ridges at the base of the beaker-shaped ridges (Fig. 5D) could have been produced by slump due to the movement of microbial flocs under wave agitation. This could have also been generated by sand chips under saltation movement over the bed surface, but that kind of movement would have created more variable depth. The asymmetrical grooves associated with these half-moon-shaped ridges do not have variable or high depths (Fig. 5F). Additionally, sand chips (shown in Fig. 3D) were not found in close vicinity to the **morphotype C/1**. It would be even easier to produce these structures in a jelly-like, freshly-grown microbial mat. Numerous patchy relicts of the **morphotype C/1** are scattered all over the bed surface (Fig. 5C, red arrow), indicating that the microbial mat-covered bed surface remained bare for a considerable time and was reasonably stabilised and lithified to some extent. In this scenario, thin veneer of microbial mat stabilising ripples crest would prevent them against reworking and flattening. Thus, movement of microbial flocs/chips under wind/wave activity cannot imprint the surface. However, it is possible to suppose that ridge-groove couplets and wrinkles present on this bedding surface may originate from the same process acting in subsurface or in intrastratal setting (Reineck 1969; Porada and Bouougri, 2007).

4.2. Morphotype C/2: Meandering grooves with sand ridges

4.2.1. Description

The structure appears mainly as meandering grooves (negative epirelief) that are sub-mm in depth and rapidly variable in width (1.5 mm on average; Fig. 6A). These structures occur on fine-grained and wave-rippled sandstone bed surfaces (Fig. 6A). The geometry of the grooves is variable and can be meandering, semicircular, or bifurcating. The groove walls are gently sloping and bounded on both sides by sand ridges of varying widths (up to 1.5 mm) and heights of approximately 2 mm (Figs 6B and C). The grooves are diverse in orientation, excluding the crests of the wave ripples, which they incise upon. Depth, width and length of the grooves measured from the outcrop are shown in Fig. 6D. Locally, they form half-loops and create triple point junctions (Fig. 6B). They also branch at multiple places (Fig. 6B). Newer grooves traverse older grooves. Patchy ripple and wrinkle structures (Figs 3A and C) are observed from the same sandstone horizon as the **morphotype C/2**.

4.2.2. Interpretation

The grooves of **morphotype C/2** may resembles cracks commonly reported from microbial mats (Fig. 3E and F) (Sarkar et al., 2006; Schieber et al., 2007). Under the influence of microbial mat cracks may develop on ripple crests such as *Manchuriophycus* but these cracks remain confined to the ripple troughs. Both types of cracks are abundantly present within the Chorhat sandstone (Fig. 3J and K) (Sarkar et al., 2014). However, the grooves under present consideration seem to have been guided by free will. They are independent of the ripple morphology with which they are associated (Table 1). These grooves are bordered by ridges, as if sand had spilled over from the grooves (Fig. 6B and C and Table 1). From these morphological details, the **morphotype C/2** resembles an animal grazing trail (Figure S10 F of Pecoits et al., 2012). However, recently Verde et al. (2022) calls into question the age of the geological formations containing these traces of Pecoits et al. (2012) by asserting a Late Paleozoic age! The traces shown in Fig. 6 from the Chorhat Sandstone are from undoubtedly of Mesoproterozoic in age (Rasmussen et al., 2002b). The similarities between the traces of Pecoits et al. (2012) and that shown in Fig. 6 of this paper include a meandering nature, additional sand of the same composition forming a ridge on the flank of the grooves, cross-cutting of pre-existing grooves, and a trend to change course. It appears that the groove-makers ploughed through loose sand, pushed aside the sand to form the ridges and formed loops, branched up and cut across older grooves in the course of their movement. The dissimilarities in sedimentological context are that traces reported by Pecoits et al. (2012) are on the planar bed surface, not on the rippled sandstone beds such as the ones shown in Fig. 6 in this paper; also, the traces reported by Pecoits et al. (2012) seemed to be more continuous than those shown Fig. 6. However, closer examination identifies some problems in accepting the structure in Fig. 6 as a "simple trail/bilaterian trail". For example, (1) the structure is not a single entity but appears to be a superimposition of many entities (see the sketch in Fig. 6), (2) the possible levees are rather irregular and laterally discontinuous or pinching out, and (3) the width of a groove is also laterally variable. The **morphotype C/2** thus cannot be interpreted as the "simple trail" of a bilaterian or even a diploblastic organism (i.e., cnidarian-grade). It can be suggested that the groove-makers moved on the sediment/water or sediment/biomat interface (Warren et al., 2020). Alternatively, microbial flocs oscillating in waves in a shallow water environment could have been responsible for generating similar structures (Warren et al., 2020). Some large protists can create multiple orientations (both parallel and transverse to ripple crest) of the grooves and their variable geometry. Tiny prokaryotes/protists similar to some of the presumed Mesoproterozoic trace fossils described by Bengtson et al. (2007) and Matz et al. (2008) were capable of moving and leaving their trails on the sediment surface. If the grooves had been created by current-swept microalgae/microbial flocs, the variable width of the grooves can be readily accounted for. Nevertheless, the freely-swinging grooves that temporarily reversed course and even formed complete loops can hardly be accounted for by the passive migration of any object or by the movement of primitive organisms under the influence of some external force, such as light, heat, or chemical gradients (El Albani et al., 2019; Matz et al., 2008; Wallraff and Wallraff, 1997). Thus, the **morphotype C/2** deserves serious consideration as a trace of early life.

5. Discussion

It has long been accepted that the earliest evolutionary record of metazoans at the base of the Cambrian merely reflects a preservation bias, not their true origin. Many researchers thus ventured into the Precambrian formations in search of metazoan records. The most spectacular findings were made in the Neoproterozoic Ediacaran series, although they possibly belonged to an exclusive group of organisms (Seilacher, 1999). However, a possible sponge ancestor was discovered in Neoproterozoic rocks (Turner, 2021). Bengtson et al. retrieved multicellular eukaryotes from another formation of the Vindhyan Supergroup that was approximately the same age as the abovementioned Chorhat Sandstone (Bengtson et al., 2009).

Nevertheless, the Precambrian motile life record must belong to the trace fossil inventory. Biomarkers suggest the appearance of eukaryotes as early as 2.7 Ga, and thus far, the oldest trace of motile organisms comes from a 2.1 Ga-old formation (El Albani et al., 2019). Even then, recognising organism traces in Precambrian terrains remains challenging, and incorrect identification can confound our understanding of the evolutionary course over time. Alternative abiogenic explanations for these presumed organism traces must be seriously considered. Two enigmatic morphotypes whose equivalents have never before been described and which can be potentially considered biogenic are discussed here

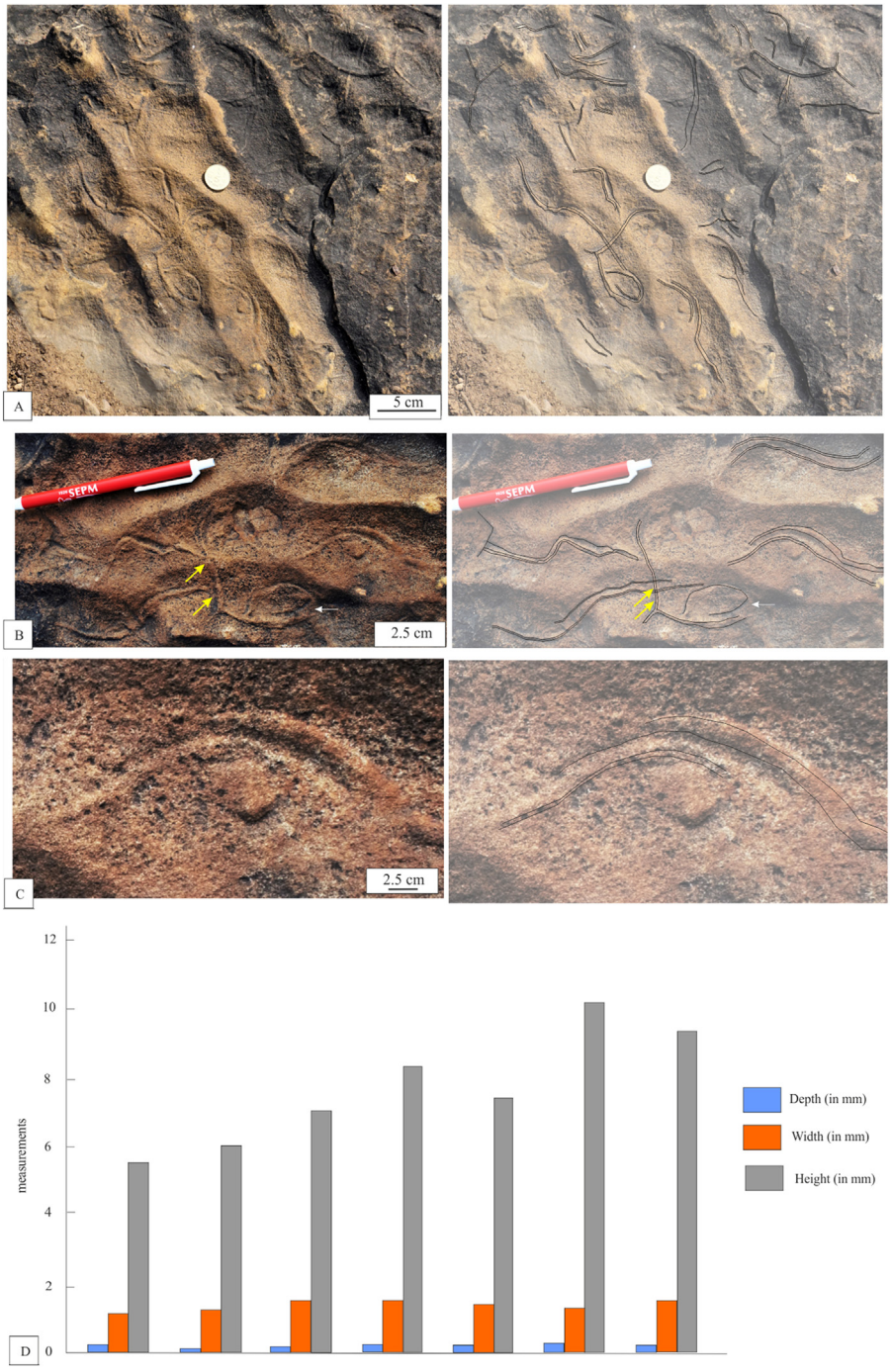

Fig. 6. Field photo of morphotype C/2 and their hand sketches for better illustration on the right hand side of each figures. A. Meandering grooves on the rippled bed surface. B. Enlarged view of the meandering grooves. Note that the grooves run without any regard for the ripple morphology. Locally, they form half-loops (white arrow) and branch up and cross-cut the older grooves (yellow arrows). C. Enlarged view of the meandering groove; note the two marginal ridges bordering the groove. D. Histogram showing variable depth, width and length of the grooves of **morphotype C/2**.
Photo de terrain du morphotype C/2 et leurs croquis pour une meilleure illustration sur le côté droit de chaque figure. A. Rainures sinueuses sur la surface du banc ondulée. B. Vue agrandie des rainures sinueuses. Les rainures se propage indépendamment de la morphologie de la ride. Localement, ils forment des demi-boucles (flèche blanche) et se ramifient en recoupant les anciens sillons (flèches jaunes). C. Vue agrandie de la rainure sinueuse; notez les deux rides marginales bordant la rainure. D. Histogramme montrant la variabilité de la profondeur, la largeur et la longueur des sillons du morphotype C/2.

(Tables 2 and 3). One thing they essentially share is a close association with profuse MRS. Thus, the role of MRS in forming and or preserving the two morphotypes discussed in this paper is very important. If MRS were not associated with these morphotypes, their features could have eroded (Sarkar et al., 2011; Warren et al., 2020). The food source was thus ready to sustain these organisms (large protists/prokaryotes/algae), had they been present. The two morphotypes examined here do not have any known equivalent in the literature but frequently occur in the studied formation. Some of the most critical components of the morphotype C/1 are the linear or curved ridges of uniform width across and along the ripple troughs. The geometry of the ridges, nonetheless, changes when the ridges run across the ripple crests. The other morphotype C/2 displays meandering grooves bordered by ridges. The grooves

Table 1
Comparison between *Manchuriophycus* and Morphotype C/2 observed in ~1.6 Ga old Chorhat Sandstone, India.
Comparaison entre Manchuriophycus *et le morphotype C/2 observé dans le grès de Chorhat datant d'environ 1,6 Ga, Inde.*

	Crack/*Manchuriophycus*	Morphotype C/2
Occurrence	Mostly occur on the bed surface of well sorted sandstone; ***Manchuriophycus*** is preferably on the ripple troughs	On the rippled sandstone bed surface; but shows no preferred occurrence in ripple troughs like ***Manchuriophycus***; run in multiple directions (some are parallel to ripple crest but some of them are also transverse in direction crosscutting ripple crest)
Length, width, depth	Length is > 15 cm (Fig. 3F); millimetres to centimetres in width; depth variable	Sub-millimetre in-depth; width is 1.5 mm, though variable within a short-range
Steepness of the side wall	Steep inclination, V-shaped in cross-section	Walls are gently inclined
Geometry/Shape	Spindle/sinuous/ptygmatic/septarian/rectangular/ birds'foot type (Choudhuri et al., 2020; McMahon et al., 2017)	Meandering, semi-circular and bifurcating grooves
Relief	Negative	Grooves are negative; ridge is positive
Presence of lateral ridges (Yes/No)	No	Yes
Nature of lateral ridges (if any)	Absent	Additional sand on the outer side of the grooves; ridges are very irregular, laterally disappearing/pinching out
Host lithology	Recorded from both siliciclastic and carbonate rocks	Observed in fine grained sandstone for the present study
In-fill material	Variable mineralogy (McMahon et al., 2017)	Fine sand for the present study
Continuity (within the limit of exposure)	Discontinuous	Discontinuous
Branching	Rarely present	Commonly present
Relationship with other features (within the limit of exposure)	Do not cross-cut each other	Cross-cuts the previous grooves

Table 2
The most common criteria considered to assess antiquity (Wacey, 2009) of the features observed from ~1.6 Ga old Chorhat Sandstone, Vindhyan Supergroup, India. Range of assessment criteria varies as below: (+++) = condition fully met; (++) = condition mostly met; (+) = condition partly met; (–) = condition not met; (~) = uncertain condition.
Les critères les plus courants utilisés pour évaluer l'ancienneté (Wacey, 2009) des caractéristiques observées dans le grès de Chorhat datant d'environ 1,6 Ga, dans le supergroupe de Vindhyan, en Inde. L'éventail des critères d'évaluation varie comme suit (+++) = condition entièrement remplie ; (++) = condition principalement remplie ; (+) = condition partiellement remplie ; (–) = condition non remplie ; (~) = condition incertaine.

		Morphotype C/1	Morphotype C/2
Criteria of antiquity	Structures must occur in rocks of known provenance (*in situ*)	+++	+++
	Structures must occur in rocks of established age, ideally dated directly by radiometric techniques	+++ (Bickford et al., 2017; Rasmussen et al., 2002a)	+++ (Bickford et al., 2017; Rasmussen et al., 2002a)
	Structures must be indigenous and syngenetic with the primary fabric of the host rock, i.e., they must be physically embedded within the rock, not introduced by post-depositional fluids	+++	+++
	Structures should not occur in high-grade metamorphic rocks	+++	+++
	The geological context of the host rock must be well understood at regional scale	+++ (Bose et al., 2001)	+++ (Bose et al., 2001)
	Fossils should not be significantly different in colour from that of the rock matrix	+++	+++
	There should be evidence for organo-sedimentary interaction	+++ (Choudhuri et al., 2020; Sarkar et al., 2006, 2016)	+++ (Choudhuri et al., 2020; Sarkar et al., 2006, 2016)

Table 3
The most common criteria considered to assess biogenicity of the features observed from ~1.6 Ga old Chorhat Sandstone, Vindhyan Supergroup, India [75]. Range of assessment criteria varies as below: (+++) = condition fully met; (++) = condition mostly met; (+) = condition partly met; (–) = condition not met; (~) = uncertain condition.
Les critères les plus courants pris en compte pour évaluer la biogénicité des caractéristiques observées dans le grès de Chorhat, datant d'environ 1,6 Ga, dans le supergroupe de Vindhyan, en Inde (Wacey, 2009). L'éventail des critères d'évaluation varie comme suit (+++) = condition entièrement remplie ; (++) = condition principalement remplie ; (+) = condition partiellement remplie ; (–) = condition non remplie ; (~) = condition incertaine.

		Morphotype C/1	Morphotype C/2
Criteria of biogenicity	Structures should exhibit biological morphology that can be related to extant cells, structures or activities	++	++
	More than a single step of biology-like processing should be evident. These steps may take the form of: biominerals (pyrite), geochemical fractionations of isotopes (sulphur and carbon), specific organic compounds	~	~
	Structures should occur within a geological context that is plausible for life, i.e., at temperatures and pressures that extant organisms are known to survive	+++	+++
	Structures should fit within a plausible evolutionary context	+++	+++
	Structures should be abundant and ideally occur in a multi-component assemblage. Ideally they should show colonial/community behaviour	+	+++

frequently change direction and thereby form loops. This morphotype is not adequately explained by the movement of microbial flocs under wave agitation or the passive migration of protozoa under the influence of an external force. Thus, the morphotype C/2 deserves serious research attention.

Nonetheless, these potential records of ancient life are particularly important because of their age of ~1.6 Ga. Although the atmospheric oxygen budget was assumed to have dropped to a minimum level between the GOE and NOE (Large et al., 2022; Lyons et al., 2014; Mukherjee et al., 2018), recent observations reveal oxy-

genated bottom waters in some localities during 1.4 Ga (Zhang et al., 2016, 2018). Furthermore, eukaryotic locomotion would have had an additional demand on the atmospheric oxygen budget (Carbone and Narbonne, 2014; Chen et al., 2019; Sperling et al., 2013). Recent experiments have confirmed that the last common ancestors of motile eukaryotes could have thrived at oxygen levels as low as 0.5% to 4% of the modern surface ocean level (Knoll and Sperling, 2014; Mills et al., 2014; Sperling et al., 2013). Additionally, oceanographic research over four decades has shown that some bilaterian animals can sustain a low O_2 concentration equivalent to 0.3% of surface ocean levels of the Mesoproterozoic average (Levin et al., 2002; Palma et al., 2005). In the background of severe oxygen scarcity, motile life (large protists/prokaryotes/algae) in the Chorhat could have utilised the oxygen produced by the photosynthetic microbiota that were abundant in the close vicinity (Gingras et al., 2011). These organisms must have had weak mobility. The oxygen scarcity must have also restricted the supply of molybdenum that is essentially required for eukaryotic growth. Whatever little Mo used to be available in the contemporary seas had been exhausted entirely in the shallow seas (Mukherjee et al., 2018; Planavsky et al., 2015). This explains the occurrence of all the potential records within the top 2 m of the shallowing-upwards Chorhat Sandstone.

6. Conclusion

The unusual morphotypes described in this work from the top of the prograding shelf succession of the 1.6 Ga-old Chorhat Sandstone might be explained by abiotic processes. Nevertheless, some are characterised by centimetre-long ridges of uniform thickness, and others are characterised by open grooves bordered by ridges that move in multiple directions, even forming loops. None of the morphotypes could be satisfactorily explained by the passive migration of any inorganic or organic masses under the influence of an external force. They could have formed by the movement of amoeba-like organisms that abundantly occurred in association with microbial mats. The preservation of such delicate features was further enhanced due to the presence of a protective microbial mat on top of the sandstone bed surfaces. Additionally, the oxygen generated by the mat-forming photosynthetic microbiota compensated for the poor atmospheric oxygen budget of the contemporary world, and thus, they confined themselves to the coastal zone. These features provide an exceptional opportunity to examine the biogenicity based on morphological characteristics, which are fundamental to the controversial debate on the biological remains from the Proterozoic Era.

Disclosure of interest

The authors have not supplied their declaration of competing interest.

Acknowledgments

All authors extend their thanks to Didier Neraudeau, the editor of the journal, Alfredo Loi and one anonymous reviewer whose comments helped to improve the manuscript. AC, SM acknowledges the Director of BSIP, Lucknow and the RDCC, BSIP for the infrastructure (**Publication no. 19/2022-23**). AC acknowledges the support offered by the staff of the University of Poitiers, La Région Nouvelle Aquitaine, and DST INSPIRE Faculty Project (**IFA 17-EAS62**), Department of Science and Technology, Govt. of India. AC also acknowledges the Department of Earth Sciences, IISER-Kolkata, where the above-mentioned project was initiated. SS acknowledges the Department of Geological Sciences, Jadavpur University for the infrastructural facility. AC, SM, and SS thank Prof. Pradip K. Bose (Jadavpur University, Kolkata, India) for scientific discussion and his comments on an earlier version of the manuscript.

References

Anbar, A.D., Knoll, A.H., 2002. Proterozoic Ocean Chemistry and Evolution: A Bioinorganic Bridge? Science 297, 1137–1142, http://dx.doi.org/10.1126/science.1069651.
Bengtson, S., Rasmussen, B., 2009. New and Ancient Trace Makers. Science 323, 346–347, http://dx.doi.org/10.1126/science.1168794.
Bengtson, S., Rasmussen, B., Krapež, B., 2007. The Paleoproterozoic megascopic Stirling biota. Paleobiology 33, 351–381, http://dx.doi.org/10.1666/04040.1.
Bengtson, S., Belivanova, V., Rasmussen, B., Whitehouse, M., 2009. The controversial "Cambrian" fossils of the Vindhyan are real but more than a billion years older. Proceddings of the National Academy of Sciences 106, 7729–7734, http://dx.doi.org/10.1073/pnas.0812460106.
Bickford, M.E., Mishra, M., Mueller, P.A., Kamenov, G.D., Schieber, J., Basu, A., 2017. U-Pb Age and Hf Isotopic Compositions of Magmatic Zircons from a Rhyolite Flow in the Porcellanite Formation in the Vindhyan Supergroup, Son Valley (India): Implications for Its Tectonic Significance. Journal of Geology 125, 367–379, http://dx.doi.org/10.1086/691186.
Bose, P.K., Chakraborty, P.P., 1994. Marine to fluvial transition: Proterozoic Upper Rewa Sandstone, Maihar, India. Sedimentary Geology 89, 285–302, http://dx.doi.org/10.1016/0037-0738(94)90098-1.
Bose, P.K., Sarkar, S., Chakrabarty, S., Banerjee, S., 2001. Overview of the meso- to neoproterozoic evolution of the Vindhyan basin, central India. Sedimentary Geology 141–142, 395–419, http://dx.doi.org/10.1016/S0037-0738(01)00084-7.
Brasier, M.D., Lindsay, J.F., 1998. A billion years of environmental stability and the emergence of eukaryotes: New data from northern Australia. Geology 26, 555–558, http://dx.doi.org/10.1130/0091-7613(1998)026<0555:ABYOES>2.3.CO;2.
Brocks, J.J., Logan, G.A., Buick, R., Summons, R.E., 1999. Archean Molecular Fossils and the Early Rise of Eukaryotes. Science 285, 1033–1036, http://dx.doi.org/10.1126/science.285.5430.1033.
Buick, R., Des Marais, D.J., Knoll, A.H., 1995. Stable isotopic compositions of carbonates from the Mesoproterozoic Bangemall group, northwestern Australia. Chemical Geology 123, 153–171, http://dx.doi.org/10.1016/0009-2541(95)00049-R.
Butterfield, N.J., 2007. Macroevolution and Macroecology Through Deep Time. Palaeontology 50, 41–55, http://dx.doi.org/10.1111/j.1475-4983.2006.00613.x.
Canfield, D.E., Poulton, S.W., Narbonne, G.M., 2007. Late-Neoproterozoic Deep-Ocean Oxygenation and the Rise of Animal Life. Science 315, 92–95, http://dx.doi.org/10.1126/science.1135013.
Canfield, D.E., Poulton, S.W., Knoll, A.H., Narbonne, G.M., Ross, G., Goldberg, T., Strauss, H., 2008. Ferruginous Conditions Dominated Later Neoproterozoic Deep-Water Chemistry. Science 321, 949–952, http://dx.doi.org/10.1126/science.1154499.
Carbone, C., Narbonne, G.M., 2014. When Life Got Smart: The Evolution of Behavioral Complexity Through the Ediacaran and Early Cambrian of NW Canada. Journal of Paleontology 88, 309–330, http://dx.doi.org/10.1666/13-066.
Chen, Z., Zhou, C., Yuan, X., Xiao, S., 2019. Death march of a segmented and trilobate bilaterian elucidates early animal evolution. Nature 573, 412–415, http://dx.doi.org/10.1038/s41586-019-1522-7.
Chen, S.-C., Sun, G.-X., Yan, Y., Konstantinidis, K.T., Zhang, S.-Y., Deng, Y., Li, X.-M., Cui, H.-L., Musat, F., Popp, D., Rosen, B.P., Zhu, Y.-G., 2020. The Great Oxidation Event expanded the genetic repertoire of arsenic metabolism and cycling. Proceedings of National Academy of Sciences 117, 10414–10421, http://dx.doi.org/10.1073/pnas.2001063117.
Choudhuri, A., 2020. Implications of microbial mat induced sedimentary structures (MISS) in carbonate rocks: An insight from Proterozoic Rohtas Limestone and Bhander Limestone, India. Journal of Earth System Sciences 129, 151, http://dx.doi.org/10.1007/s12040-020-01416-x.
Choudhuri, A., Banerjee, S., Sarkar, S., 2020. A review of biotic signatures within the Precambrian Vindhyan Supergroup: Implications on evolution of microbial and metazoan life on Earth. Journal of Mineralogical and Petrological Sciences 115, 162–174, http://dx.doi.org/10.2465/jmps.190827a.
Collinson, J.D., Thompson, D.B., 1989. Sedimentary Structures, 2nd ed. Unwin Hyman, London, Boston, Sydney, Wellington.
Cunningham, J.A., Liu, A.G., Bengtson, S., Donoghue, P.C.J., 2017. The origin of animals: Can molecular clocks and the fossil record be reconciled? BioEssays 39, http://dx.doi.org/10.1002/bies.201600120 (e201600120).
De, C., 2006. Ediacara fossil assemblage in the upper Vindhyans of Central India and its significance. Journal of Asian Earth Science 27, 660–683, http://dx.doi.org/10.1016/j.jseaes.2005.06.006.
Donoghue, P.C.J., Benton, M.J., 2007. Rocks and clocks: calibrating the Tree of Life using fossils and molecules. Trends in Ecology and Evolution 22, 424–431, http://dx.doi.org/10.1016/j.tree.2007.05.005.
dos Reis, M., Thawornwattana, Y., Angelis, K., Telford, M.J., Donoghue, P.C.J., Yang, Z., 2015. Uncertainty in the Timing of Origin of Animals and the Limits of Precision in Molecular Timescales. Current Biology 25, 2939–2950, http://dx.doi.org/10.1016/j.cub.2015.09.066.
El Albani, A., Mangano, M.G., Buatois, L.A., Bengtson, S., Riboulleau, A., Bekker, A., Konhauser, K., Lyons, T., Rollion-Bard, C., Bankole, O., Lekele Baghekema, S.G., Meunier, A., Trentesaux, A., Mazurier, A., Aubineau, J., Laforest, C., Fontaine,

C., Recourt, P., Chi Fru, E., Macchiarelli, R., Reynaud, J.Y., Gauthier-Lafaye, F., Canfield, D.E., 2019. Organism motility in an oxygenated shallow-marine environment 2.1 billion years ago. Proceedings of National Academy of Sciences 116, 3431–3436, http://dx.doi.org/10.1073/pnas.1815721116.

Eriksson, P.G., Sarkar, S., Samanta, P., Banerjee, S., Porada, H., Catuneanu, O., 2010. Paleoenvironmental Context of Microbial Mat-Related Structures in Siliciclastic Rocks. In: Seckbach, J., Oren, A. (Eds.), Microbial Mats: Modern and Ancient Microorganisms in Stratified Systems, Cellular Origin, Life in Extreme Habitats and Astrobiology. Springer, Netherlands, Dordrecht, pp. 71–108, http://dx.doi.org/10.1007/978-90-481-3799-2_5.

Erwin, D.H., 2015. Early metazoan life: divergence, environment and ecology. Philosophical Transations of Royal Society B Biological Sciences 370, 20150036, http://dx.doi.org/10.1098/rstb.2015.0036.

Erwin, D.H., 2020. The origin of animal body plans: a view from fossil evidence and the regulatory genome. Development 147, http://dx.doi.org/10.1242/dev.182899 (dev182899).

Erwin, D.H., Laflamme, M., Tweedt, S.M., Sperling, E.A., Pisani, D., Peterson, K.J., 2011. The Cambrian Conundrum: Early Divergence and Later Ecological Success in the Early History of Animals. Science 334, 1091–1097, http://dx.doi.org/10.1126/science.1206375.

Gingras, M., Hagadorn, J.W., Seilacher, A., Lalonde, S.V., Pecoits, E., Petrash, D., Konhauser, K.O., 2011. Possible evolution of mobile animals in association with microbial mats. Nature Geosciences 4, 372–375, http://dx.doi.org/10.1038/ngeo1142.

Grundvåg, S.-A., Jelby, M.E., Olaussen, S., Śliwińska, K.K., 2021. The role of shelf morphology on storm-bed variability and stratigraphic architecture, Lower Cretaceous, Svalbard. Sedimentology 68, 196–237, http://dx.doi.org/10.1111/sed.12791.

Javaux, E.J., Lepot, K., 2018. The Paleoproterozoic fossil record: Implications for the evolution of the biosphere during Earth's middle-age. Earth Science Reviews 176, 68–86, http://dx.doi.org/10.1016/j.earscirev.2017.10.001.

Knoll, A.H., 2014. Paleobiological Perspectives on Early Eukaryotic Evolution. Cold Spring Harbour Perspective Biology 6, a016121, http://dx.doi.org/10.1101/cshperspect.a016121.

Knoll, A.H., Sperling, E.A., 2014. Oxygen and animals in Earth history. Proceedings of National Academy of Sciences 111, 3907–3908, http://dx.doi.org/10.1073/pnas.1401745111.

Large, R.R., Hazen, R.M., Morrison, S.M., Gregory, D.D., Steadman, J.A., Mukherjee, I., 2022. Evidence that the GOE was a prolonged event with a peak around 1900 Ma. Geosystems & Geoenvironment 1, 100036, http://dx.doi.org/10.1016/j.geogeo.2022.100036.

Levin, L., Gutiérrez, D., Rathburn, A., Neira, C., Sellanes, J., Muñoz, P., Gallardo, V., Salamanca, M., 2002. Benthic processes on the Peru margin: a transect across the oxygen minimum zone during the 1997-98 El Niño. Progress in Oceanography 53, 1–27, http://dx.doi.org/10.1016/S0079-6611(02)00022-8.

López-García, P., Moreira, D., 2008. Tracking microbial biodiversity through molecular and genomic ecology. Research in Microbiology 159, 67–73, http://dx.doi.org/10.1016/j.resmic.2007.11.019.

López-García, P., Moreira, D., 2021. Physical connections: prokaryotes parasitizing their kin. Environmental Microbiological Reports 13, 54–61, http://dx.doi.org/10.1111/1758-2229.12910.

Lozano-Fernandez, J., dos Reis, M., Donoghue, P.C.J., Pisani, D., 2017. Rel-Time Rates Collapse to a Strict Clock When Estimating the Timeline of Animal Diversification. Genome Biology and Evolution 9, 1320–1328, http://dx.doi.org/10.1093/gbe/evx079.

Lyons, T.W., Reinhard, C.T., Planavsky, N.J., 2014. The rise of oxygen in Earth's early ocean and atmosphere. Nature 506, 307–315, http://dx.doi.org/10.1038/nature13068.

Mänd, K., Lalonde, S.V., Robbins, L.J., Thoby, M., Paiste, K., Kreitsmann, T., Paiste, P., Reinhard, C.T., Romashkin, A.E., Planavsky, N.J., Kirsimäe, K., Lepland, A., Konhauser, K.O., 2020. Palaeoproterozoic oxygenated oceans following the Lomagundi–Jatuli Event. Nature Geosciences 13, 302–306, http://dx.doi.org/10.1038/s41561-020-0558-5.

Mandal, S., Choudhuri, A., Mondal, I., Sarkar, S., Chakraborty, P.P., Banerjee, S., 2019. Revisiting the boundary between the Lower and Upper Vindhyan, Son valley, India. Journal of Earth System Sciences 128, 222, http://dx.doi.org/10.1007/s12040-019-1250-2.

Mandal, S., Roy Choudhury, T., Das, A., Sarkar, S., Banerjee, S., 2022. Shallow marine glauconitization during the Proterozoic in response to intrabasinal tectonics: A study from the Proterozoic Lower Bhander Sandstone, Central India. Precambrian Research 372, 106596, http://dx.doi.org/10.1016/j.precamres.2022.106596.

Matz, M.V., Frank, T.M., Marshall, N.J., Widder, E.A., Johnsen, S., 2008. Giant Deep-Sea Protist Produces Bilaterian-like Traces. Current Biology 18, 1849–1854, http://dx.doi.org/10.1016/j.cub.2008.10.028.

McMahon, S., Smeerdijk Hood, A.V., Mcilroy, D., 2017. **The origin and occurrence of subaqueous sedimentary cracks**. In: Brasier, A.T., McIlroy, D., McLoughlin, N.) (Eds.), **Earth System Evolution and Early Life: A Celebration of the Work of Martin Brasier**. Geol. Soc, London, pp. 285–309.

Mills, D.B., Ward, L.M., Jones, C., Sweeten, B., Forth, M., Treusch, A.H., Canfield, D.E., 2014. Oxygen requirements of the earliest animals. Proceedings of National Academy of Sciences 111, 4168–4172, http://dx.doi.org/10.1073/pnas.1400547111.

Mukherjee, I., Large, R.R., Corkrey, R., Danyushevsky, L.V., 2018. The Boring Billion, a slingshot for Complex Life on Earth. Scientific Reports 8, 4432, http://dx.doi.org/10.1038/s41598-018-22695-x.

Noffke, N., Awramik, S.M., 2013. Stromatolites and MISS—Differences between relatives. GSA Today 23, 4–9, http://dx.doi.org/10.1130/GSATG187A.1.

Och, L.M., Shields-Zhou, G.A., 2012. The Neoproterozoic oxygenation event: Environmental perturbations and biogeochemical cycling. Earth Science Reviews 110, 26–57, http://dx.doi.org/10.1016/j.earscirev.2011.09.004.

Palma, M., Quiroga, E., Gallardo, V.A., Arntz, W., Gerdes, D., Schneider, W., Hebbeln, D., 2005. Macrobenthic animal assemblages of the continental margin off Chile (22° to 42°S). Journal of the Marine Biological Association of the United Kingdom 85, 233–245, http://dx.doi.org/10.1017/S0025315405011112h.

Partin, C.A., Bekker, A., Planavsky, N.J., Scott, C.T., Gill, B.C., Li, C., Podkovyrov, V., Maslov, A., Konhauser, K.O., Lalonde, S.V., Love, G.D., Poulton, S.W., Lyons, T.W., 2013. Large-scale fluctuations in Precambrian atmospheric and oceanic oxygen levels from the record of U in shales. Earth Planetary Science Letters 369–370, 284–293, http://dx.doi.org/10.1016/j.epsl.2013.03.031.

Pecoits, E., Konhauser, K.O., Aubet, N.R., Heaman, L.M., Veroslavsky, G., Stern, R.A., Gingras, M.K., 2012. Bilaterian Burrows and Grazing Behavior at >585 Million Years Ago. Science 336, 1693–1696, http://dx.doi.org/10.1126/science.1216295.

Peterson, K.J., Lyons, J.B., Nowak, K.S., Takacs, C.M., Wargo, M.J., McPeek, M.A., 2004. Estimating metazoan divergence times with a molecular clock. Proceedings of National Academy of Sciences 101, 6536–6541, http://dx.doi.org/10.1073/pnas.0401670101.

Peterson, K.J., Cotton, J.A., Gehling, J.G., Pisani, D., 2008. The Ediacaran emergence of bilaterians: congruence between the genetic and the geological fossil records. Philosophical Transactions of Royal Society B Biological Sciences 363, 1435–1443, http://dx.doi.org/10.1098/rstb.2007.2233.

Pisani, D., Liu, A.G., 2015. Animal Evolution: Only Rocks Can Set the Clock. Current Biology 25, R1079–R1081, http://dx.doi.org/10.1016/j.cub.2015.10.015.

Planavsky, N.J., Tarhan, L.G., Bellefroid, E.J., Evans, D.A.D., Reinhard, C.T., Love, G.D., Lyons, T.W., 2015. Late Proterozoic Transitions in Climate, Oxygen, and Tectonics, and the Rise of Complex Life. The Paleontological Society Papers 21, 47–82, http://dx.doi.org/10.1017/S1089332600002965.

Rasmussen, B., Bengtson, S., Fletcher, I.R., McNaughton, N.J., 2002a. Discoidal Impressions and Trace-Like Fossils More Than 1200 Million Years Old. Science 296, 1112–1115, http://dx.doi.org/10.1126/science.1070166.

Rasmussen, B., Bose, P.K., Sarkar, S., Banerjee, S., Fletcher, I.R., McNaughton, N.J., 2002b. 1.6 Ga U-Pb zircon age for the Chorhat Sandstone, lower Vindhyan, India: Possible implications for early evolution of animals. Geology 30, 103–106, http://dx.doi.org/10.1130/0091-7613(2002)030<0103:GUPZAF>2.0.CO;2.

Robbins, L.J., Lalonde, S.V., Planavsky, N.J., Partin, C.A., Reinhard, C.T., Kendall, B., Scott, C., Hardisty, D.S., Gill, B.C., Alessi, D.S., Dupont, C.L., Saito, M.A., Crowe, S.A., Poulton, S.W., Bekker, A., Lyons, T.W., Konhauser, K.O., 2016. Trace elements at the intersection of marine biological and geochemical evolution. Earth Science Reviews 163, 323–348, http://dx.doi.org/10.1016/j.earscirev.2016.10.013.

Sarkar, S., Banerjee, S., 2020. A Synthesis of Depositional Sequence of the Proterozoic Vindhyan Supergroup in Son Valley: A Field Guide, Springer Geology. Springer, Singapore, http://dx.doi.org/10.1007/978-981-32-9551-3.

Sarkar, S., Banerjee, S., Samanta, P., Jeevankumar, S., 2006. Microbial mat-induced sedimentary structures in siliciclastic sediments: Examples from the 1.6 Ga Chorhat Sandstone, Vindhyan Supergroup, M.P., India. Journal of Earth System Sciences 115, 49–60, http://dx.doi.org/10.1007/BF02703025.

Sarkar, S., Banerjee, S., Samanta, P., Chakraborty, N., Chakraborty, P.P., Mukhopadhyay, S., Singh, A.K., 2014. Microbial mat records in siliciclastic rocks: Examples from Four Indian Proterozoic basins and their modern equivalents in Gulf of Cambay. Journal of Asian Earth Sciences 91, 362–377, http://dx.doi.org/10.1016/j.jseaes.2014.03.002.

Sarkar, S., Choudhuri, A., Mandal, S., Eriksson, P.G., 2016. Microbial mat-related structures shared by both siliciclastic and carbonate formations. Journal of Palaeogeography 5, 278–291, http://dx.doi.org/10.1016/j.jop.2016.05.001.

Sarkar, S., Samanta, P., Altermann, W., 2011. Setulfs, modern and ancient: Formative mechanism, preservation bias and palaeoenvironmental implications. Sedimentary Geology 238, 71–78, http://dx.doi.org/10.1016/j.sedgeo.2011.04.003.

Schieber, J., Bose, P.K., Eriksson, P.G., Banerjee, S., Sarkar, S., Altermann, W., Catuneanu, O., 2007. Atlas of Microbial Mat Features Preserved within the Siliciclastic Rock Record. Elsevier.

Scott, C., Lyons, T.W., Bekker, A., Shen, Y., Poulton, S.W., Chu, X., Anbar, A.D., 2008. Tracing the stepwise oxygenation of the Proterozoic ocean. Nature 452, 456–459, http://dx.doi.org/10.1038/nature06811.

Seilacher, A., 1999. Biomat-related lifestyles in the Precambrian. Palaios 14, 86–93, http://dx.doi.org/10.2307/3515363.

Seilacher, A., 2007. Trace Fossil Analysis. Springer, Berlin, Heidelberg, http://dx.doi.org/10.1007/978-3-540-47226-1.

Seilacher, A., Bose, P.K., Pflüger, F., 1998. Triploblastic Animals More Than 1 Billion Years Ago: Trace Fossil Evidence from India. Science 282, 80–83, http://dx.doi.org/10.1126/science.282.5386.80.

Sharma, M., Shukla, Y., 2009. Taxonomy and affinity of Early Mesoproterozoic megascopic helically coiled and related fossils from the Rohtas Formation, the Vindhyan Supergroup, India. Precambrian Research 173, 105–122, http://dx.doi.org/10.1016/j.precamres.2009.05.002.

Shields-Zhou, G., Och, L., 2011. The case for a neoproterozoic oxygenation event: Geochemical evidence and biological consequences. GSA Today 21, 4–11, http://dx.doi.org/10.1130/GSATG102A.1.

Sperling, E.A., Halverson, G.P., Knoll, A.H., Macdonald, F.A., Johnston, D.T., 2013. A basin redox transect at the dawn of animal life. Earth Planetary Science Letters 371–372, 143–155, http://dx.doi.org/10.1016/j.epsl.2013.04.003.

Srivastava, P., 2012. Problematic fossils from the Palaeo-Neoproterozoic Vindhyan Supergroup, India. Arabian Journal of Geosciences 5, 1411–1422, http://dx.doi.org/10.1007/s12517-011-0315-6.
Summons, R.E., Jahnke, L.L., Hope, J.M., Logan, G.A., 1999. 2-Methylhopanoids as biomarkers for cyanobacterial oxygenic photosynthesis. Nature 400, 554–557, http://dx.doi.org/10.1038/23005.
Tripathy, G.R., Singh, S.K., 2015. Re–Os depositional age for black shales from the Kaimur Group, Upper Vindhyan, India. Chemical Geology 413, 63–72, http://dx.doi.org/10.1016/j.chemgeo.2015.08.011.
Turner, E.C., 2021. Possible poriferan body fossils in early Neoproterozoic microbial reefs. Nature 596, 87–91, http://dx.doi.org/10.1038/s41586-021-03773-z.
Verde, M., Netto, R.G., Azurica, D., Lavina, E.L., Di Pasquo, M., 2022. Revisiting the supposed oldest bilaterian trace fossils from Uruguay: Late Paleozoic, not Ediacaran. Palaeogeography Palaeoclimatology Palaeoecology 602, 111158, http://dx.doi.org/10.1016/j.palaeo.2022.111158.
Wacey, D., 2009. **Early Life on Earth. A Practical Guide**. Springer, pp. 274.
Wallraff, E., Wallraff, H.G., 1997. Migration and bidirectional phototaxis in Dictyostelium discoideum slugs lacking the actin cross-linking 120 kDa gelation factor. Journal of Experimental Biology 200, 3213–3220, http://dx.doi.org/10.1242/jeb.200.24.3213.
Warren, L.V., Buatois, L.A., Mángano, M.G., Simões, M.G., Santos, M.G.M., Poiré, D.G., Riccomini, C., Assine, M.L., 2020. Microbially induced pseudotraces from a Pantanal soda lake, Brazil: Alternative interpretations for Ediacaran simple trails and their limits. Geology 48, 857–861, http://dx.doi.org/10.1130/G47234.1.
Zhang, S., Wang, X., Wang, H., Bjerrum, C.J., Hammarlund, E.U., Costa, M.M., Connelly, J.N., Zhang, B., Su, J., Canfield, D.E., 2016. Sufficient oxygen for animal respiration 1,400 million years ago. Proceedings of National Academy of Sciences 113, 1731–1736, http://dx.doi.org/10.1073/pnas.1523449113.
Zhang, K., Zhu, X., Wood, R.A., Shi, Y., Gao, Z., Poulton, S.W., 2018. Oxygenation of the Mesoproterozoic ocean and the evolution of complex eukaryotes. Nature Geosciences 11, 345350, http://dx.doi.org/10.1038/s41561-018-0111-y.